• Review •

Prospects and challenges in augmented reality displays

Yun-Han LEE, Tao ZHAN, Shin-Tson WU*

College of Optics & Photonics, University of Central Florida, Orlando, FL 32816, USA

*** Corresponding author,** swu@creol.ucf.edu

Received: 5 December 2018 **Accepted:** 17 December 2018

Supported by Air Force Office of Scientific Research (FA9550-14-1-0279); Goertek Electronics.

Citation: Yun-Han LEE, Tao ZHAN, Shin-Tson WU. Prospects and challenges in augmented reality displays. Virtual Reality & Intelligent Hardware, 2019, 1(1): 10—20
DOI: 10.3724/SP.J.2096-5796.2018.0009

Abstract Augmented reality (AR) displays are attracting significant attention and efforts. In this paper, we review the adopted device configurations of see-through displays, summarize the current development status and highlight future challenges in micro-displays. A brief introduction to optical gratings is presented to help understand the challenging design of grating-based waveguide for AR displays. Finally, we discuss the most recent progress in diffraction grating and its implications.

Keywords Near-eye displays; See-through display; Augmented reality; Micro-displays; Bragg gratings

1 Introduction

Augmented reality (AR) displays are highly anticipated as the next-generation display devices. In a glasses-like form-factor, the seamless overlay between computer-generated information and the physical world will enrich human interaction with both physical and digital world. In this paper, we first review the major configurations of AR displays adopted in present commercialized or near-commercialized products, and then discuss the advances and challenges on the micro-displays and grating couplers.

2 Construction of major AR displays

The basic construction of major AR displays includes a display unit, magnifying optics, and a combiner to overlay displayed content and physical world[1]. Based on the type of combiners, AR devices can be categorized into partial-mirror and grating-based configurations (Figure 1).

A typical example of partial-mirror based AR devices is the Google Glass™[2,3], where a beam splitter cube is utilized as the combiner in Figure 1(a). The magnifying optics is a reflective concave mirror disposed directly on the beam-splitter cube. This configuration provides the simplest solution to AR glasses with larger form-factor. Figure 1(b) shows another configuration utilizing a free-form partial reflector[4,5] both as a magnifying optics and a combiner, eliminating the need for additional magnifying optics (e. g., Mira™, Meta 2™ and DreamGlass™). An interesting configuration adopted by NED AR™ utilizes a free-form prism for achieving glasses-like form-factor in Figure 1(c). This configuration sophisticatedly incorporates two refraction surfaces, a total-internal-reflection surface, and a partial reflection surface into one element, and therefore allows extra design freedom[6–9], reducing device size with minimal sacrifice on image quality and field of view (FOV). A correcting prism is necessary to cancel the refraction of the ambient light from the main free-form prism. To further reduce size, partial reflector

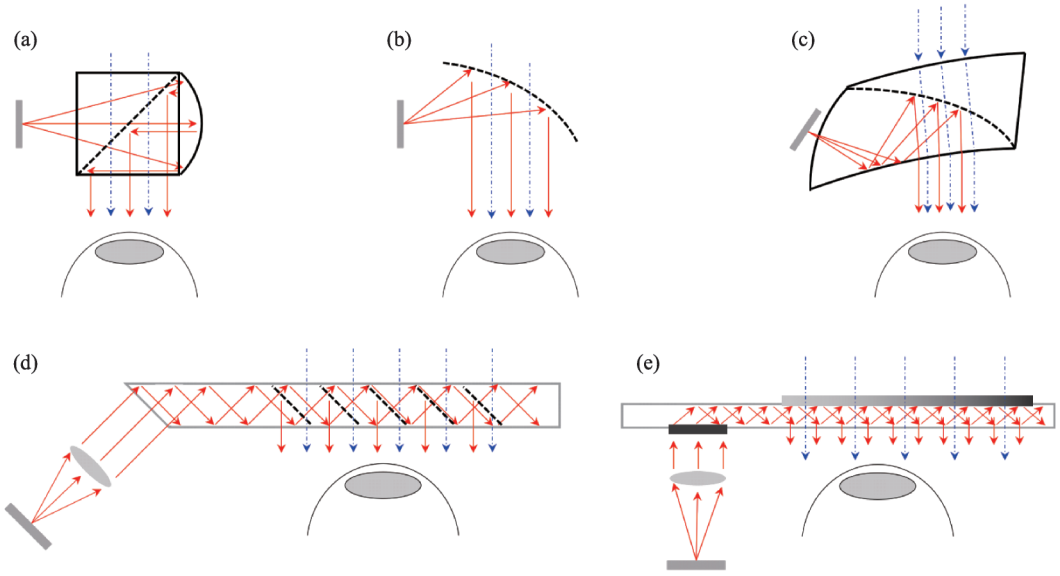

Figure 1 Adopted configurations of AR glasses. (a)-(d) Partial-mirror based ARs; (e) A grating-based AR. Dashed black lines: partial reflectors; Red arrows: display optical path; Blue arrows: see-through optical path.

array in Figure 1(d) is devised (e.g., Lumus™)[10-15]. In this configuration, the thickness of combiner optics can be further reduced. The see-through transmittance is also improved as the reflectance of each partial mirror is reduced to distribute light over a larger eye box. This design sacrifices the FOV due to the limited angular range allowed in the waveguide. The image quality would also be decreased as multiple reflections could result in stray light and non-uniform intensity. In general, the optical quality and efficiency in partial-reflector based AR are higher, and yet the form-factor tends to be larger than a regular pair of glasses, except for the partial mirror array configuration.

Grating-based waveguide AR devices[16-18] utilize diffraction to guide the display light through a thin glass plate (the "waveguide") whose thickness ranges from 0.3mm to 1mm. As shown in Figure 1(e), in general, an input-coupling grating is deployed at the display end to diffract input light to an angle larger than the critical angle. The diffracted light will then travel toward viewing region through total internal reflection (TIR). An output-coupling grating is deployed in front of the eye to diffract TIR-guided light such that it travels toward the viewer. To distribute light over a larger eye box, low-efficiency gratings (leaky gratings) with gradient efficiency is usually employed; the process of distributing light across wide eye box is referred to as exit-pupil expansion or pupil replication. Both the dispersive nature of gratings and multiple diffractions post challenges for achieving large FOV and uniform output intensity. This manifests as obvious non-uniformity in color across FOV typically when a white image is displayed. To achieve better uniformity, the overall efficiency is often compromised. Despite the inferior display quality, the pursuit for smaller form-factor still draws wide attention for grating-based waveguide AR devices.

3 Advances in micro-displays

As a see-through device, AR displays post strict requirement on display brightness. For partial-mirror based ARs, the efficiency can be as high as 50%, while for grating-based waveguide ARs, the efficiency can be as low as 10%. To establish a quantitative guideline, ambient contrast ratio (ACR) is defined as[19,20]:

$$ACR = \frac{L_{on} + L_{ambient} \cdot T}{L_{off} + L_{ambient} \cdot T} \tag{1}$$

where T is see-through transmittance, L_{on} (L_{off}) represents on- (off-) state luminance (nits) while $L_{ambient}$ is the

ambient luminance. In general, ambient lighting condition is measured in illuminance (lux); for comparison, we translate illuminance to luminance by dividing a factor of π (i.e., ambient light scattered from a perfectly white paper). For instance, in a normal living room, the illuminance is around 100lux, and thus it is translated to $L_{ambient}$ ≅30nits, while in a regular office, $L_{ambient}$≅150nits. For outdoors, on an overcast day, $L_{ambient}$≅300nits, and $L_{ambient}$≅3000nits on a sunny day.

Even for a high contrast display (L_{on}/L_{off}>100), ambient light can wash out the content and renders the image unrecognizable. A general rule requires a minimum ACR of 3:1 for recognizable images, an ACR of 5:1 for adequate readability and an ACR over 10:1 for appealing quality[20]. Therefore, for an AR glass with T=90%, in an office lighting condition, the target luminance level through the device should be at least 550 nits in order to achieve ACR=5:1.

Due to the maturity of projection displays, liquid-crystal-on-silicon (LCoS) is the first choice for micro-displays in AR glasses. LCoS is a high-resolution reflective display. In this type of displays, light emitting diodes (LEDs) are used as light source, and the light is reflected by a polarizing beam splitter (PBS). Upon reflection toward LCoS, the polarization is modulated and reflected toward the PBS, which translates the phase retardation of each pixel into intensity and therefore generates images. Because the driving circuit is hidden beneath the mirror, small pixel sizes (<5μm) with a large aperture ratio (>93%) can be achieved. Also, the advancement in LED technology enables high-luminance LCoS (3×10^4nits)[21,22], these advantages lead to their early adoption in Google Glass, HoloLens and Magic Leap One AR glasses. The major disadvantage is the requirement for a polarizing beam splitter, preventing further decrease in form-factor. Similar to LCoS, digital light processing (DLP) is also a reflective display utilizing the switching of micro-mirrors to generate images. They can also provide high brightness with a reflective configuration[23]. Although a polarizing beam splitter is not needed, the reflective optical path still has a relatively large form factor. This type of technology is adopted in Vuzix Blade™.

To further reduce form factor, emissive displays are being evaluated for their potential in replacing LCoS or DLP. Although organic light emitting diodes (OLEDs) have been widely implemented in smartphones, smartwatches, and several virtual reality headsets, their lifetime degrades significantly at higher brightness level, making them unsuitable to drive at the same luminance level as the reflective displays. At the current stage, 5000-nit luminance level can be attained for full-color OLED micro-displays[24,25].

To achieve high brightness, micro-LED displays are being heavily investigated. In recent advances, over 10^6nit peak luminance has been reported[26−29]. The major challenges with micro-LEDs include mass-transfer yield, non-uniform pixel brightness, high cost and decreased external quantum efficiency at smaller die size (a drop of 50% when reducing pixel size to 5μm[29]). If these technical challenges can be successfully overcome, micro-LED could be a disruptive display technology for AR glasses.

To compare ACR, let us assume a partial mirror of 50% transmittance and a waveguide device of 10% or 20% overall efficiency. If a micro-display has 4X extension in eye-box along both directions, then the brightness would be divided by a factor of 16. With these assumptions, the ambient contrast ratio in office ambient (150nits) is compared in Table 1.

In this estimation, the current OLED brightness in any case cannot achieve an ACR of 5:1. This makes OLED displays unsuitable for compact AR glasses without significant improvement in brightness. Using LCoS/DLP as display modules, for partial-mirror AR glasses, the brightness is more than enough due to the high overall efficiency (~50%) and 50% blockage of the ambient light. For waveguide ARs, at an overall efficiency of 10%, the ACR is quite insufficient with the inherent high see-through transmittance. An additional light shield is required to reduce ambient transmittance for readability. At 30%

Table 1 The ACR comparing different AR configurations

Characteristic			LCoS/DLP	micro-OLED	micro-LED
Luminance at display output/nits			3×10^4	5×10^3	10^{6*}
Partial-mirror ARs, η=50%	Luminance at eye box/nits		937.5	156.3	31250
	ACR@500 lux, T=50%		13.5	3.1	417.7
Waveguide ARs, η=10%	Luminance at eye box/nits		187.5	31.3	6250
	ACR@500 lux	T=90%	2.4	1.2	47.3
		T=50%	3.5	1.4	84.3
		T=30%	5.2	1.7	139.9
Waveguide ARs, η=20%	Luminance at eye box/nits		375.0	62.5	12500
	ACR@500 lux	T=90%	3.8	1.5	93.6
		T=50%	6.0	1.8	167.7
		T=30%	9.3	2.4	278.8

*micro-LED is still under active development. The listed luminance level only serves as a reference. η: Overall efficiency.

transmittance, the brightness is reasonably sufficient. This results in sunglasses-like appearance. If the overall efficiency is increased to 20%, higher see-through transmittance over 50% can be allowed. Apparently, before micro-LED displays become widely available, boosting overall efficiency is a crucial subject for grating-based waveguide AR glasses.

4 Advances in grating couplers

Through magnification optics, the display light will be collimated and then coupled into a waveguide through a diffraction grating. Different from the convention in integrated photonics, the term "waveguide" here refers to a transparent, flat glass or plastic whose thickness ranges from 0.3mm to 1mm.

The critical angle of TIR posts a limit on the shallowest angle light may travel within the waveguide. Also, it is preferred to maintain the steepest angle less than 80° to prevent gaps between each two TIRs. As such, material for high-index waveguide is also a critical topic to attain a wider angular range. The current commercially available glasses have a refractive index as high as 2.0, while plastics can have a refractive index around 1.75. Although high index materials can essentially increase the FOV to over 50°×50°, the pursuit of large-FOV posts critical challenges in output uniformity due to the diffractive nature of gratings.

To understand the difficulties in achieving high-quality grating-based ARs, it is worthwhile to investigate the basics of diffraction gratings. Gratings represent periodic modulation of refractive index. When light passes through a typical grating, it will diffract into multiple orders (directions). The first-order diffraction angle can be described by

$$\sin\theta_{\text{in}} - \sin\theta_{\text{out}} = \frac{m\lambda}{n\Lambda_x} \tag{2}$$

where θ_{in} represents the incident angle, θ_{out} represents the diffracted angle, m is the order of diffraction, n is the refractive index and Λ_x is the horizontal periodicity.

Equation (2) states the wavelength dependency on diffraction angle. If the same grating is used for RGB colors, they will be diffracted into different angular range, and yet the allowable angular range limited by the waveguide is the same for RGB. Therefore, if the grating is optimized for the green wavelength to have the widest FOV, then the red and blue colors will be cut and have narrower FOV. To have the same FOV, three different gratings are needed to diffract RGB lights into the same nominal angle. A three-grating single-waveguide design is reported by Mukawa et al.[18]. However, in this design, cross-talk between different primaries (e.g., red light being diffracted by the grating designated for green light) become an

issue. Low cross-talk single waveguide design is often achieved by reducing spectral bandwidth of grating couplers and thereby sacrificing the overall efficiency. To maintain high efficiency, two- and three-waveguide designs are being utilized[30]; however, in this case, the thickness is compromised.

Several factors in the coupling process make the uniform distribution of outcoupled intensity over large FOV a tough challenge. Firstly, light from different pixel travels at different angles in the waveguide. This translates to different travel distances between each TIR, and thus different total number of TIR across the out-coupler. Also, the spectral bandwidth results in an angular spread for each pixel. Finally, for gratings with lower index modulation ($\delta n<0.1$), diffraction spectra for different pixels are different. Due to these reasons, designing a uniform exit-pupil expansion at all angles is exceedingly difficult, especially when the desired FOV is large. Although reducing overall efficiency will contribute to uniformity, low optical throughput is undesirable as mentioned in the previous section.

4.1 Volume bragg gratings

Two major types of gratings are utilized as input and output couplers: volume Bragg gratings (VBGs) and surface-relief gratings (SRGs). Sony™ promoted VBGs in Figure 2(a) for application as grating combiners[31−33]. VBGs are fabricated by differential polymerization of monomer precursors under interference exposure, and they exhibit small sinusoidal index modulation ($\delta n\leqslant 0.05$) across the volume. Due to the high spectral selectivity, reflective VBGs allow for single-waveguide design[18], and they exhibit superior see-through quality. However, the spectral selectivity leads to lower efficiency as only a minor portion of the display light is utilized. Although VBG materials with a large δn were demonstrated[34], they are comparatively more sensitive to environmental stimuli such as temperature or humidity.

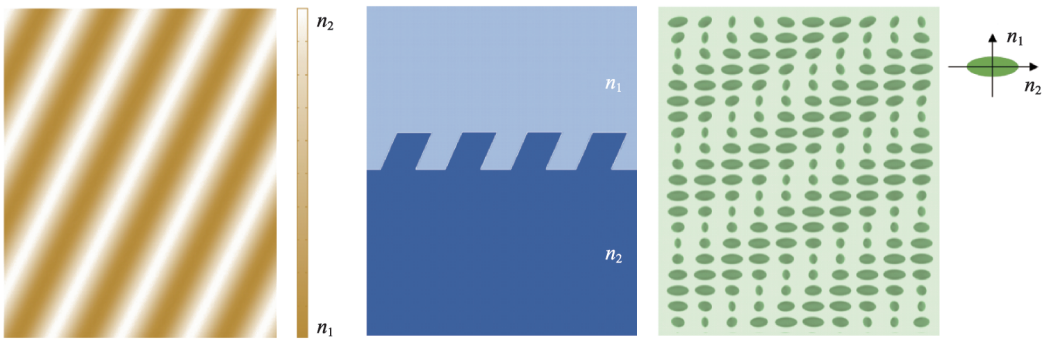

Figure 2 Three major types of gratings. (a) Volume Bragg grating; (b) Surface-relief grating; (c) Polarization volume grating.

Another interesting type of VBGs promoted by Digilens™ is based on holographic polymer-dispersed liquid crystals (HPDLCs; Figure 3)[35−39], which employs phase separation of LCs and monomers to create index modulation with interference exposure. After exposure, the LC nano-droplets formed in the grating structure can be driven by an applied voltage, allowing the realization of electrically switchable VBGs.

4.2 Surface-relief gratings

Nokia™ and Microsoft™ promoted the use of SRGs as combiners in Figure 2(b)[40−44]. In this type of gratings, a master mold is first defined by interference and then subjected to ion-beam etching at an oblique angle to create slanted binary features[41]. The feature on the prepared master mold is replicated onto polymer materials by nanoimprint for mass production. As a result of high index contrast between air and polymer, large binary index modulation can be achieved ($\delta n\geqslant 0.5$). To reduce δn for design purpose,

other polymer material can be utilized to substitute air. In Figure 4(a) and 4(b), we compare the performances of two input-coupling gratings: transmissive SRG (δn=0.7, d=0.27μm) and reflective VBG (δn=0.05, d=15μm). As discussed before, the high angular/spectral selectivity makes it possible to adopt the single-waveguide design with low-δn VBGs. On the other hand, high δn SRGs exhibits ultra-wide spectral and angular bandwidth, making it advantageous for high overall efficiency comparing to VBGs. The wide bandwidth also makes it necessary to adopt three-waveguide design to prevent crosstalk between primary colors. Due to the advancement in nanoimprint, mass replication of high-efficiency transmissive SRGs and low-efficiency reflective SRGs is proven viable[30].

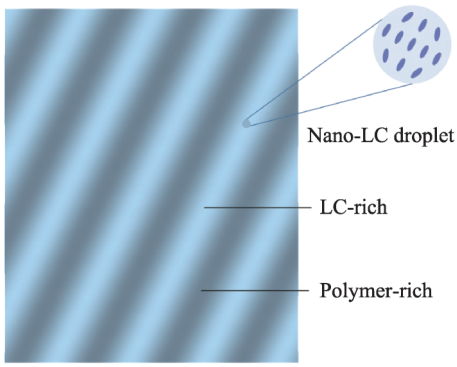

Figure 3 Electrically-switchable VBG: holographic polymer-dispersed liquid crystals.

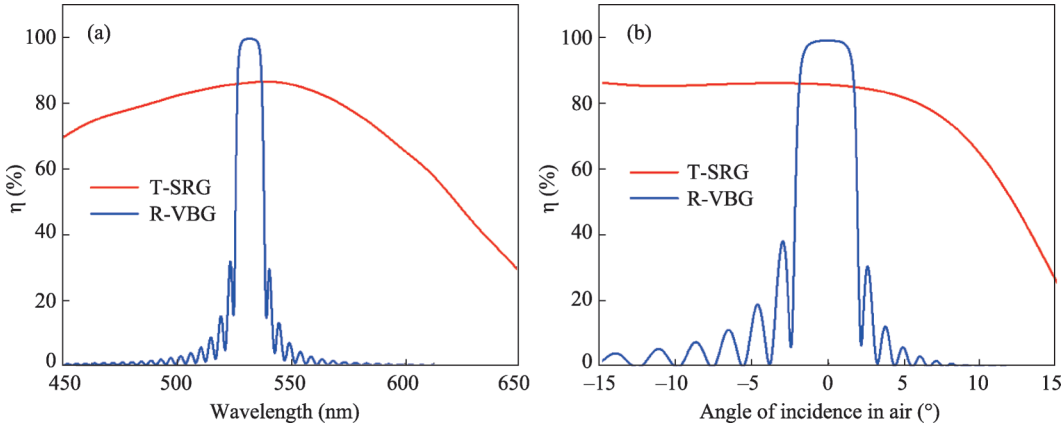

Figure 4 Simulated (a) spectral and (b) angular performance of transmissive SRG (δn=0.7, d=0.27 μm) and reflective VBG (δn=0.05, d=15 μm) for input-coupling gratings.

4.3 Polarization volume gratings

While VBGs and SRGs are well-developed and adopted for commercial products, a different type of Bragg grating based on liquid crystals (LCs), called polarization volume gratings (PVGs; Figure 2(c)), is demonstrated in recent years[45–52]. Two methods can be used for fabricating PVGs. The first method utilizes photo-alignment and self-assembly of the LC material[46,47,50]: a photo-alignment layer is first coated onto the desired substrate, and then the coated substrate is subjected to interference exposure to define the in-plane crystal axis. Liquid crystal polymer precursor is then coated onto the exposed photo-alignment layer. The chiral agent in the precursor promotes the self-assembly of LCs into a helical structure following the recorded grating periodicity on the photo-alignment layer and formed PVGs. The other method[52] utilizes the photocycloaddition of cinnamate moieties to record the volumetric polarization field into the material: a film of LC precursor containing cinnamic ester groups is first coated onto a substrate. The coated sample is subjected to interference exposure of left-handed and right-handed polarized lights, and the three-dimensional polarization field is recorded. After annealing at elevated temperature, the birefringence increases and a PVG is formed. With either method, instead of index variation, Bragg diffraction of PVGs is based on the helical rotation in LC optical axis. This means the effective index modulation δn is essentially the birefringence (Δn) of the LC material. Due to the heavy investment of LCD industry, wide

selection of Δn ranging from 0.05 to 0.4 is available. Besides high-efficiency and large diffraction angle, reflective PVGs show unique polarization selectivity regardless of the modulation factor (product of δn, wave vector *k*, and grating thickness *d*). As illustrated in Figure 5, only circularly polarized light with the same handedness to the helical rotation will be diffracted (in this case, right-handed), while light with the opposite handedness will pass through.

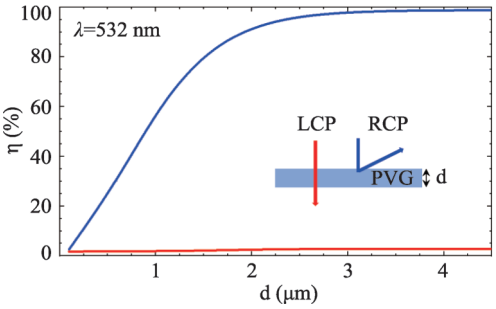

Figure 5 Efficiency for RCP and LCP of a PVG with Δn=0.15, horizontal period of 440 nm, vertical period of 205nm and central wavelength of 532nm.

High polarization selectivity introduces new designs[53]. It may be utilized for boosting efficiency[54], increasing FOV[55] and alternative exit-pupil expansion design[56]. As shown in Figure 6, instead of utilizing gradient efficiency, an alternative exit-pupil expansion design utilizes polarization management and polarization selectivity to distribute the output light[56]. In such design, a liquid crystal layer is disposed to control the polarization state, as the optical axis and thickness of LC layer can be easily controlled, the polarization state can also be controlled such that at every interaction with the out-coupling PVG, a similar amount of light is diffracted across the eye box. This allows distribution of light without introducing non-uniform see-through transmittance and adds new free parameters for optimization of exit pupil expansion.

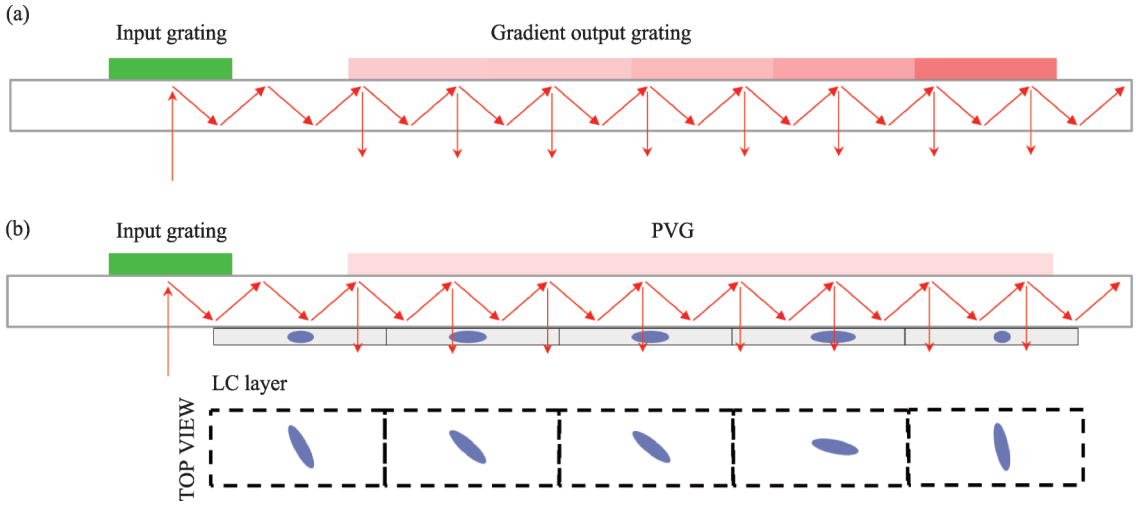

Figure 6 An illustration of exit-pupil expansion based on (a) gradient output grating and (b) polarization control. Instead of gradient output efficiency, an additional LC layer is utilized to control the polarization state and thereby distribute light evenly at each interaction with the polarization selective PVG.

5 Conclusion

In conclusion, we have reviewed major configurations for AR displays. While grating-based ARs provide the slimmest geometry, a major improvement needs to be made in the optical throughput and display brightness. The dispersive nature of gratings and the consequent intensity/color non-uniformity is also a critical issue to be addressed. We also reviewed the optical properties and advantages of VBGs and SRGs and presented a newly developed PVG. With unique polarization selectivity, PVGs open new design space and serve as a potential candidate for achieving efficient and uniform throughput AR displays.

References

1 Cakmakci O, Rolland J. Head-worn displays: a review. Journal of Display Technology, 2006, 2(3): 199–216
DOI:10.1109/JDT.2006.879846

2 Cado H, Moliton R. Polarization splitter, method of manufacturing same and ophthalmic lens incorporating projection inserts containing it. U.S. Patent, 0136082.A1, 2004–7–15

3 Martinez M A, Saeedi E, Amirparviz B. Head-mounted display including integrated projector. U.S. Patent, 9128285.B2, 2005–9–8

4 Wang J, Liang Y, Xu M. Design of a see-through head-mounted display with a freeform surface. Journal of the Optical Society of Korea, 2015, 19(6): 614–618
DOI:10.3807/JOSK.2015.19.6.614

5 Pulli K. Meta 2: immersive optical-see-through augmented reality. IEEE SigPort, 2017, 48(1): 132–133

6 Takahashi K. Head or face mounted image display apparatus. U.S. Patent, 5701202, 1997–12–23

7 Yamazaki S, Inoguchi K, Saito Y, Morishima H, Taniguchi N. Thin wide-field-of-view HMD with free-form-surface prism and applications. Proc SPIE, 1999, 3639: 453–462
DOI:10.1117/12.349411

8 Cheng D, Wang Y, Chang J. Design of a lightweight and wide field-of-view HMD system with freeform surface prism. Infrared and Laser Engineering, 2007, 36 (3): 309–311

9 Cheng D, Wang Y, Hua H, Talha M M. Design of an optical see-through head-mounted display with a low f-number and large field of view using a freeform prism. Applied Optics, 2009, 48(14): 2655–2668
DOI:10.1364/AO.48.002655

10 Amitai Y. A two - dimensional aperture expander for ultra - compact, high - performance head - worn displays. SID International Symposium Digest of Techninal Papers, 2005, 36(1): 360–363
DOI: 10.1889/1.2036446

11 Amitai Y. Substrate-guided optical device utilizing thin transparent layer. U.S. Patent, 772443.B2, 2010–5–25

12 Cheng D, Wang Y, Xu C, Song W, Jin G. Design of an ultra-thin near-eye display with geometrical waveguide and freeform optics. Optics Express, 2014, 22(17): 20705–20719
DOI:10.1364/OE.22.020705

13 Wang Q, Cheng D, Hou Q, Hu Y, Wang Y. Stray light and tolerance analysis of an ultrathin waveguide display. Applied Optics, 2015, 54(28): 8354–8362
DOI:10.1364/AO.54.008354

14 Gu L, Cheng D, Wang Q, Hou Q, Wang Y. Design of a two-dimensional stray-light-free geometrical waveguide head-up display. Applied Optics, 2018, 57(31): 9246–9256
DOI: 10.1364/AO.57.009246

15 Frommer A. Lumus optical technology for AR. SID International Symposium Digest of Techninal Papers , 2017, 48(1): 134–135
DOI:10.1002/sdtp.11589

16 Amitai Y, Reinhorn S, Friesem A A. Visor-display design based on planar holographic optics. Applied Optics, 1995, 34 (8): 1352-1356
DOI:10.1364/AO.34.001352

17 Levola T. Diffractive optics for virtual reality displays. SID International Symposium Digest of Techninal Papers , 2006, 14(5): 467–475
DOI:10.1889/1.2206112

18 Mukawa H, Akutsu K, Matsumura I, Nakano S, Yoshida T, Kuwahara M, Aiki K. A full-color eyewear display using planar waveguides with reflection volume holograms. SID International Symposium Digest of Techninal Papers, 2009, 17(3): 185–193
DOI:10.1889/JSID17.3.185

19 Dobrowolski J A, Sullivan B T, Bajcar R C. Optical interference, contrast-enhanced electroluminescent device. Applied Optics, 1992, 31(28): 5988−5996
DOI:10.1364/AO.31.005988

20 Chen H, Tan G, Wu S T. Ambient contrast ratio of LCDs and OLED displays. Optics Express, 2017, 25(26): 33643−33656
DOI:10.1364/OE.25.033643

21 Handschy M A, McNeil J R, Weissman P E. Ultrabright head-mounted displays using LED-illuminated LCOS. In: Helmet-and Head-Mounted Displays XI: Technologies and Applications. International Society for Optics and Photonics, 2006, 62240S
DOI:10.1117/12.668481

22 Huang Y, Liao E, Chen R, Wu S-T. Liquid-Crystal-on-Silicon for Augmented Reality Displays, 2018, 8(12): 2366
DOI:10.3390/app8122366

23 Pettitt G, Ferri J, Thompson J. Practical application of TI DLP® technology in the next generation head-up display system. SID International Symposium Digest of Techninal Papers, 2015, 46(1): 700−703
DOI:10.1002/sdtp.10269

24 Haas G. Microdisplays for augmented and virtual reality. SID International Symposium Digest of Techninal Papers, 2018, 49(1): 506−509
DOI:10.1002/sdtp.12445

25 Ghosh A, Donoghue E P, Khayrullin I, Ali T, Wacyk l, Tice K, Vazan F, Prache O, Wang Q, Sziklas L, Fellowes D, Draper R. Ultra-High-Brightness 2K×2K full-color OLED microdisplay using direct patterning of OLED emitters. SID International Symposium Digest of Techninal Papers, 2017, 48(1): 226−229
DOI:10.1002/sdtp.11674

26 El-Ghoroury H S, ChuangC-L, Alpaslan Z Y. Quantum photonic imager (QPI): A novel display technology that enables more than 3D applications. SID International Symposium Digest of Techninal Papers, 2015, 46(1): 371−374
DOI:10.1002/sdtp.10255

27 Templier F. GaN-based emissive microdisplays: A very promising technology for compact, ultra-high brightness display systems. Journal of the Society for Information Display, 2016, 24(11): 669−675
DOI:10.1002/jsid.516

28 Zhang L, Ou F, Chong W C, Chen Y, Li Q. Wafer-scale monolithic hybrid integration of Si-based IC and III−V epi-layers—A mass manufacturable approach for active matrix micro-LED micro-displays. Journal of the Society for Information Display, 2018, 26(3): 137−145
DOI:10.1002/jsid.649

29 Olivier F, Daami A, Dupré L, Henry F, Aventurier B, Templier F. 25-4: investigation and improvement of 10μm Pixel-pitch GaN-based Micro-LED arrays with very high brightness. SID International Symposium Digest of Techninal Papers, 2017, 48(1): 353−356
DOI:10.1002/sdtp.11615

30 Kress B C, Cummings W J. Towards the ultimate mixed reality experience: HoloLens display architecture choices. SID International Symposium Digest of Techninal Papers, 2017, 48 (1): 127−131
DOI:10.1002/sdtp.11586

31 Solymar L, Cooke D J. Volume Holography and Volume Gratings. Academic press, 1981

32 Gleeson M R, Sheridan J T. A review of the modelling of free-radical photopolymerization in the formation of holographic gratings. Journal of Optics A: Pure and Applied Optics, 2009, 11(2): 24008
DOI:10.1088/1464-4258/11/2/024008

33 BruderF-K, Fäcke T, Hagen R, Hönel D, Orselli E, Rewitz C, Rölle T, Walze G. Diffractive optics with high Bragg selectivity: volume holographic optical elements in Bayfol® HX photopolymer film. In: Optical Systems Design 2015: Optical Design and Engineering VI. International Society for Optics and Photonics, 2015, 96260T
DOI: 10.1117/12.2191587

34 Rasmussen T. Overview of high-efficiency transmission gratings for molecular spectroscopy. Spectroscopy, 2014, 29(4):

32–39

35 Sutherland R L, Natarajan L V, Tondiglia V P, Bunning T J. Bragg gratings in an acrylate polymer consisting of periodic polymer-dispersed liquid-crystal planes. Chemistry of Materials, 1993, 5(10): 1533–1538
DOI:10.1021/cm00034a025

36 Sutherland R L, Tondiglia V P, Natarajan L V, Bunning T J, Adams W W. Electrically switchable volume gratings in polymer-dispersed liquid crystals. Applied Physics Letters, 1994, 64(9): 1074–1076
DOI:10.1063/1.110936

37 Sutherland R L. Polarization and switching properties of holographic polymer-dispersed liquid-crystal gratings. I. Theoretical model. Journal of the Optical Society of America B, 2002, 19(12): 2995–3003
DOI:10.1364/JOSAB.19.002995

38 Liu Y J, Sun X W. Holographic polymer-dispersed liquid crystals materials, formation, and applications. Advances in OptoElectronics, 2008, 1: 684349
DOI:10.1155/2008/684349

39 Waldern J D, Grant A J, Popovich M M. DigiLens AR HUD waveguide technology. SID International Symposium Digest of Techninal Papers, 2018, 49 (1): 204–207
DOI:10.1002/sdtp.12523

40 Moharam M G, Pommet D A, Grann E B, Gaylord T K. Stable implementation of the rigorous coupled-wave analysis for surface-relief gratings: enhanced transmittance matrix approach. Journal of the Optical Society of America A, 1995, 12(5): 1077–1086
DOI:10.1364/JOSAA.12.001077

41 Levola T, Laakkonen P. Replicated slanted gratings with a high refractive index material for in and outcoupling of light. Optics Express, 2007, 15(5): 2067–2074
DOI:10.1364/OE.15.002067

42 Laakkonen P, Siitonen S, Levola T, Kuittinen M. High efficiency diffractive incouplers for light guides. In: Integrated Optics: Devices, Materials, and Technologies XII. International Society for Optics and Photonics, 2008, 68960E
DOI:10.1117/12.768666

43 Äyräs P, Saarikko P, Levola T. Exit-pupil expander with a large field of view based on diffractive optics. Journal of the Society for Information Display, 2009, 17(8): 659–664
DOI:10.1889/JSID17.8.659

44 Bai B, Laukkanen J, Kuittinen M, Siitonen S. Optimization of nonbinary slanted surface-relief gratings as high-efficiency broadband couplers for light guides. Applied Optics, 2010, 49(28): 5454–5464
DOI:10.1364/AO.49.005454

45 Weng Y, Xu D, Zhang Y, Li X, Wu S-T. Polarization volume grating with high efficiency and large diffraction angle. Optics Express, 2016, 24(16): 17746–17759
DOI:10.1364/OE.24.017746

46 Gao K, McGinty C, Payson H, Berry S, Vornehm J, Finnemeyer V, Roberts B, Bos P. High-efficiency large-angle pancharatnam phase deflector based on dual-twist design. Optics Express, 2017, 25(6): 6283-6293
DOI:10.1364/OE.25.006283

47 Xiang X, Kim J, Komanduri R, Escuti M J. Nanoscale liquid crystal polymer Bragg polarization gratings. Optics Express, 2017, 25(16): 19298-19308
DOI:10.1364/OE.25.019298

48 Kobashi J, Yoshida H, Ozaki M. Planar optics with patterned chiral liquid crystals. Nature Photonics, 2016(10): 389
DOI:10.1038/nphoton.2016.66

49 Kobashi J, Mohri Y, Yoshida H, Ozaki M. Circularly-polarized, large-angle reflective deflectors based on periodically patterned cholesteric liquid crystals. Optical Data Processing and Storage, 2017, 3(1): 61–66
DOI:10.1515/odps-2017-0008

50 Lee Y H, Yin K, Wu S T. Reflective polarization volume gratings for high efficiency waveguide-coupling augmented reality displays. Optics Express, 2017, 25 (22): 27008–27014

DOI:10.1364/OE.25.027008

51 Lee Y H, Tan G, Zhan T, Weng Y, Liu G, Gou F, Peng F, Tabiryan N V, Gauza S, Wu S T. Recent progress in Pancharatnam-Berry phase optical elements and the applications for virtual / augmented realities. Optical Data Processing and Storage, 2017, 3(1): 79–88
DOI:10.1515/odps-2017-0010

52 Sakhno O, Gritsai Y, Sahm H, Stumpe J. Fabrication and performance of efficient thin circular polarization gratings with Bragg properties using bulk photo-alignment of a liquid crystalline polymer. Applied Physics B, 2018, 124(3): 52
DOI:10.1007/s0034

53 Äyräs P, Saarikko P. Near-to-eye display based on retinal scanning and a diffractive exit-pupil expander. In: Optics, Photonics, and Digital Technologies for Multimedia Applications. International Society for Optics and Photonics, 2010, 77230V

54 Pasi L, Nicolas P, Jari T. Diffractive optics for mobile solutions: light incoupling and polarization control with light guides. Japanese Journal of Applied Physics, 2008, 47(8S1): 6635

55 Shi Z, Chen W T, Capasso F. Wide field-of-view waveguide displays enabled by polarization-dependent metagratings. In: Digital Optics for Immersive Displays. International Society for Optics and Photonics, 2018, 1067615.
DOI:10.1117/12.2315635

56 Lee Y H, Tan G, Yin K, Zhan T, Wu S T. Compact see-through near-eye display with depth adaption. Journal of the Society for Information Display, 2018, 26(2): 64–70
DOI:10.1002/jsid.635